Effect of the image potential on the binding energy of excitons in semiconductor quantum wells

1991 J. Phys.: Condens. Matter 3 9907

(http://iopscience.iop.org/0953-8984/3/49/007)

J. Phys.: Condens. Matter 3 (1991) 9907–9914. Printed in the UK

Effect of the image potential on the binding energy of excitons in semiconductor quantum wells

L Wendler† and B Hartwig

Institut für Festkörpertheorie und Theoretische Optik, Friedrich-Schiller-Universität Jena, Max-Wien-Platz 1, D/O-6900 Jena, Federal Republic of Germany

Received 18 September 1990, in final form 2 July 1991

Abstract. We report the results of variational estimates of the binding energy of excitons in quantum wells along the effect of the image potential.

In recent years optical properties of semiconductor quantum wells have received considerable research interest both experimentally and theoretically. Measurements on absorption coefficients of interband excitons in these structures showed clear evidence of multiple subbands due to the quantum confinement of electrons and holes by the band-edge discontinuities at the heterointerface (see e.g. Dingle *et al* 1974, 1975, Miller *et al* 1981, 1984, Meynadier *et al* 1985). Most of the attention has been focused on the excitons formed between the lower-lying electron and hole subbands, the latter being split into heavy-hole and light-hole subbands. It has been well established that the binding energies of excitons in lower-dimensional structures are significantly enhanced from the values in bulk materials as a result of the confined carrier motion. Most of the theoretical determinations of the exciton binding energy performed so far used variational calculations (see e.g. Lee and Lin 1979, Miller *et al* 1981, Bastard *et al* 1982, Greene and Bajaj 1983, Greene *et al* 1984, Brum and Bastard 1985, Wu 1989). Whittaker and Elliot (1988) and Tran Thoai *et al* (1990) calculated the exciton binding energy by numerical integration of the Schrödinger equation. Recently experimental measurements of the exciton binding energy in dependence on the well width of GaAs–$Ga_{1-x}Al_xAs$ quantum wells have been reported by Koteles and Chi (1988).

In this paper we present a variational calculation in the effective-mass approximation of the exciton binding energy in semiconductor quantum wells along to the effects of the image potential. The effects arise due to the different polarizabilities of the semiconductors forming the semiconductor microstructure.

The Hamiltonian of the Wannier exciton in semiconductors with zincblende structure such as GaAs and $Ga_{1-x}Al_xAs$ is expressed in terms of a 6×6 matrix. In GaAs and $Ga_{1-x}Al_xAs$, however, the exciton Hamiltonian can be further reduced to a 4×4 matrix as the value of the spin–orbit splitting is much larger than the exciton binding energy. Due to reduction in symmetry (along the axis of growth) and the band discontinuities at the heterointerfaces the degeneracy of the valence band at

† Permanent address: Institut für Theoretische Physik, Technische Universität Merseburg, Geusaer Straße, D/O-4200 Merseburg, Federal Republic of Germany.

0953-8984/91/499907+08$03.50

the Γ point is removed. Following, the contribution of the off-diagonal terms to the binding energy is rather small. Hence, it is possible to retain only the diagonal part of the hole Hamiltonian (Greene *et al* 1984). This means that light-hole and heavy-hole excitons are uncoupled. In the framework of effective-mass approximation, the Hamiltonian of the Wannier exciton using cylindrical coordinates in the x–y plane is given by (Greene *et al* 1984, Brum and Bastard 1985)

$$H = -\frac{\hbar^2}{2\mu_\pm}\left[\frac{1}{r}\frac{\partial}{\partial r}\left(r\frac{\partial}{\partial r}\right)+\frac{1}{r^2}\frac{\partial^2}{\partial\varphi^2}\right]-\frac{\hbar^2}{2m_e}\frac{\partial^2}{\partial z_e^2}+V_e(z_e)$$
$$-\frac{\hbar^2}{2m_{h\pm}}\frac{\partial^2}{\partial z_h^2}+V_h(z_h)+V^C(r;z_e,z_h) \tag{1}$$

where m_e is the effective mass of the conduction electron, $m_{h\pm}$ the heavy (+) or light (−) hole effective mass along the direction perpendicular to the heterointerface, and $\mu_\pm$ is the corresponding reduced exciton mass in the x–y plane. Both, $m_{h\pm}$ and $\mu_\pm$ are expressed in terms of the Luttinger parameters γ_1 and γ_2 as $m_{h\pm}{}^{-1} = m_0{}^{-1}(\gamma_1 \mp 2\gamma_2)$, $\mu_\pm{}^{-1} = m_e{}^{-1} + m_0{}^{-1}(\gamma_1 \pm \gamma_2)$ where m_0 is the free electron mass. The position of the electron and the hole are designated by $\boldsymbol{x}_e$ and $\boldsymbol{x}_h$, respectively, and (r,φ) are the relative coordinates in the x–y plane. $V_e(z_e)$ is the confining potential for the electrons in the conduction band and $V_h(z_h)$ that for the holes of the valence band, $V^C(r;z_e,z_h)$ is the electron–hole interaction potential in the quantum well. The quantum well considered here is realized by a double heterostructure (DHS) consisting of a smaller gap semiconductor ($\nu = 1$) for $a > z > 0$ (for instance GaAs) which is symmetrically embedded between a wider gap semiconductor ($\nu = 2$) for $z > a$ and $0 > z$ (for instance $Ga_{1-x}Al_xAs$).

The trial wave function used in the variational calculation of the exciton binding energy is

$$\psi(\boldsymbol{x}_e,\boldsymbol{x}_h) = \sum_{K,K'} \varphi_K^e(z_e)\,\varphi_{K'}^h(z_h)\,g_{KK'}(\boldsymbol{x}_e,\boldsymbol{x}_h). \tag{2}$$

Here we assume that the Hamiltonian H is dominated by V_e and V_h. Hence, we use the assumption of the strong confinement limit which is valid if $a < a_{ex\pm}$ (where $a_{ex\pm} = 4\pi\epsilon_0\epsilon_{s1}\hbar^2/e^2\mu_\pm$ is the bulk exciton Bohr radius and ϵ_{s1} the static dielectric constant of semiconductor 1). For simplicity we use $g_{KK'}(\boldsymbol{x}_e,\boldsymbol{x}_h) = g(r,\varphi)$. The separability in r,φ and z_e,z_h of $\psi(\boldsymbol{x}_e,\boldsymbol{x}_h)$ has been shown to lead to accurate results for GaAs–$Ga_{1-x}Al_xAs$ quantum wells with thicknesses ranging from about 3 to about 30 nm (Brum and Bastard 1985). The function $\varphi_K^e(z_e)$ and $\varphi_{K'}^h(z_h)$ are the envelope wave functions of electrons and holes defined by the corresponding single-particle Schrödinger equations. Within the square well potential with infinite barrier the envelope wave functions are given by

$$\varphi_K^{e,h}(z_{e,h}) = \sqrt{\frac{2}{a}}\ \sin\left(\frac{\pi(K+1)}{a}z\right) \tag{3}$$

and the corresponding energy eigenvalues, the subband energies, are

$$\mathcal{E}_K^{e,h\pm} = \frac{\pi^2\hbar^2}{2m_{e,h\pm}\,a^2}(K+1)^2 \qquad K = 0,1,2,\ldots\ . \tag{4}$$

The wave function $g(r,\varphi)$ describes the internal motion of the exciton parallel to the interfaces. Using equations (2)–(4) in the Schrödinger equation of the exciton one obtains

$$\left[-\frac{\hbar^2}{2\mu_\pm}\left(\frac{1}{r}\frac{\partial}{\partial r}\left(r\frac{\partial}{\partial r}\right)+\frac{1}{r^2}\frac{\partial^2}{\partial\varphi^2}\right)+V^{\mathrm{C}}_{KK'}(r)\right]g(r,\varphi)=\mathcal{E}^{KK'}_{\pm}g(r,\varphi)\,. \tag{5}$$

Herein the matrix element of the electron–hole interaction potential is given by

$$V^{\mathrm{C}}_{KK'}(r)=\int \mathrm{d}z_{\mathrm{e}}\int \mathrm{d}z_{\mathrm{h}}\,[\varphi^{\mathrm{e}}_{K}(z_{\mathrm{e}})]^2\,[\varphi^{\mathrm{h}}_{K'}(z_{\mathrm{h}})]^2 V^{\mathrm{C}}(r;z_{\mathrm{e}},z_{\mathrm{h}})\,. \tag{6}$$

We minimize the expection value $E^{KK'}(\lambda)=\langle g|H|g\rangle / \langle g|g\rangle$ and obtain by this variational procedure the exciton binding energy $E_{\mathrm{B}}{}^{KK'}=-\min E_{\pm}{}^{KK'}(\lambda)$, this being the rigorous upper bound for the true binding energy. For $g(r,\varphi)$ we use the 1s-like trial function

$$g_{1s}(r)=N\exp\left(-\frac{\lambda r}{a_{\mathrm{ex}\pm}}\right) \tag{7}$$

with λ the variational parameter and N a normalization constant.

With respect to the bulk case, the electron–hole interaction is modified by image effects arising from the different polarizabilities of the semiconductors of the layered system. To calculate the electron–hole interaction potential we solve at first Poisson's equation together with the boundary conditions of electrostatics and in a second step we calculate the electrostatic energy for an electron–hole pair at the positions $\boldsymbol{x}_{\mathrm{e}}$ and $\boldsymbol{x}_{\mathrm{h}}$. The interaction potential is given by

$$\begin{aligned}V^{\mathrm{C}}(r;z_{\mathrm{e}},z_{\mathrm{h}})=\frac{1}{2\pi}\int_0^\infty \mathrm{d}q_\parallel\; q_\parallel\,\{J_0(q_\parallel r)\,[V^{\mathrm{DIR}}(q_\parallel;z_{\mathrm{e}},z_{\mathrm{h}})+V^{\mathrm{MIM}}(q_\parallel;z_{\mathrm{e}},z_{\mathrm{h}})]\\ +V^{\mathrm{SIM}}(q_\parallel,z_{\mathrm{e}})+V^{\mathrm{SIM}}(q_\parallel,z_{\mathrm{h}})\}\end{aligned} \tag{8}$$

with J_0 being the Bessel function of the first kind, $q_\parallel=|\boldsymbol{q}_\parallel|$ the absolute value of the wavevector $\boldsymbol{q}_\parallel$ in the x–y plane and $V^{\mathrm{C}}(q_\parallel;z_{\mathrm{e}},z_{\mathrm{h}})$ is the two-dimensional Fourier transform of $V^{\mathrm{C}}(r;z_{\mathrm{e}},z_{\mathrm{h}})$. We write the matrix elements in the form

$$V^{\mathrm{C}}_{KK'}(q_\parallel)=-\frac{\mathrm{e}^2}{2\epsilon_0\epsilon_{s1}q_\parallel}f_{KK'}(q_\parallel) \tag{9}$$

where the form factors $f_{KK'}(q_\parallel)$ are calculated according equation (7) to be

$$f_{KK'}(q_\parallel)=\int \mathrm{d}z_{\mathrm{e}}\int \mathrm{d}z_{\mathrm{h}}\,[\varphi^{\mathrm{e}}_{K}(z_{\mathrm{e}})]^2\,[\varphi^{\mathrm{h}}_{K'}(z_{\mathrm{h}})]^2\,f(q_\parallel;z_{\mathrm{e}},z_{\mathrm{h}})\,. \tag{10}$$

The contributions to the form factor $f(q_\parallel;z_{\mathrm{e}},z_{\mathrm{h}})$ are (Wendler *et al* 1990)

$$f^{\mathrm{DIR}}(q_\parallel;z_{\mathrm{e}},z_{\mathrm{h}})=\mathrm{e}^{-q_\parallel|z_{\mathrm{e}}-z_{\mathrm{h}}|} \tag{11}$$

$$\begin{aligned}f^{\mathrm{MIM}}(q_\parallel;z_{\mathrm{e}},z_{\mathrm{h}})=\epsilon_{s12}\frac{\mathrm{e}^{-q_\parallel(a-z_{\mathrm{e}})}+\epsilon_{s12}\mathrm{e}^{-q_\parallel(a+z_{\mathrm{e}})}}{\mathrm{e}^{q_\parallel a}-\epsilon^2_{s12}\mathrm{e}^{-q_\parallel a}}\mathrm{e}^{q_\parallel z_{\mathrm{h}}}\\ +\epsilon_{s12}\frac{\mathrm{e}^{q_\parallel(a-z_{\mathrm{e}})}+\epsilon_{s12}\mathrm{e}^{-q_\parallel(a-z_{\mathrm{e}})}}{\mathrm{e}^{q_\parallel a}-\epsilon^2_{s12}\mathrm{e}^{-q_\parallel a}}\mathrm{e}^{-q_\parallel z_{\mathrm{h}}}\end{aligned} \tag{12}$$

and

$$f^{\mathrm{SIM}}(q_\parallel, z_{e,h}) = \frac{\epsilon_{s12}}{e^{q_\parallel a} - \epsilon_{s12}^2 e^{-q_\parallel a}} \frac{1}{2} \left(e^{-q_\parallel (a-2z_{e,h})} + e^{q_\parallel (a-2z_{e,h})} + 2\epsilon_{s12} e^{-q_\parallel a}\right) \tag{13}$$

where $\epsilon_{s12} = (\epsilon_{s1} - \epsilon_{s2})/(\epsilon_{s1} + \epsilon_{s2})$. The interaction potential includes two physical different parts, the direct coulomb part equation (11) and the image parts equations (12) and (13). The image contribution to the interaction potential itselfs consists of two parts. The mutual image (MIM) potential arises from the two charges of the electron and hole. The image charge of the electron interacts with the charge of the hole and vice versa. But the self-image (SIM) potential of the electron and that of the hole arise from their image charges alone. This means interaction of the charge of the electron (hole) with its image charge. According to this physical origin the self-image potential doesn't depend on the difference r between the electron and the hole in the x–y plane. But for large distances r between the electron and the hole in the x–y plane, both the direct and the mutual image parts go to zero. Further, one can easily obtain from the above equations that for $a \to \infty$ both image contributions vanish as in the case $\epsilon_{s2} \to \epsilon_{s1}$. In all explicit estimations we restrict ourselves to the lowest optical subband transition $K' = 0 \to K = 0$. For this case the form factor $f_{00}(q_\parallel)$ is given by

$$f_{00}^{\mathrm{DIR}}(q_\parallel) = \frac{q_\parallel a}{(q_\parallel a)^2 + (2\pi)^2} + \frac{1}{q_\parallel a} - 2(q_\parallel a)^2 (1 - e^{-q_\parallel a}) \times \left\{ \frac{(2\pi)^2}{(q_\parallel a)^2 [(q_\parallel a)^2 + (2\pi)^2]} \right\} \tag{14}$$

$$f_{00}^{\mathrm{MIM}}(q_\parallel) = \frac{1 - e^{-q_\parallel a}}{1 - \epsilon_{s12}^2 e^{-2q_\parallel a}} (2\epsilon_{s12} + 2\epsilon_{s12}^2 e^{-q_\parallel a}) \times \left(\frac{1}{(q_\parallel a)^2} - \frac{2}{(q_\parallel a)^2 + (2\pi)^2} + \frac{(q_\parallel a)^2}{[(q_\parallel a)^2 + (2\pi)^2]^2} \right) \tag{15}$$

$$f_{00}^{\mathrm{SIM}}(q_\parallel) = \frac{\epsilon_{s12}}{1 - \epsilon_{s12}^2 e^{-2q_\parallel a}} \left[2\epsilon_{s12} + (1 - e^{-2q_\parallel a}) \left(\frac{1}{q_\parallel a} - \frac{q_\parallel a}{(q_\parallel a)^2 + \pi^2} \right) \right]. \tag{16}$$

In figure 1 the interaction potential $V^{\mathrm{C}}{}_{00}(r)$ is plotted for a GaAs–$Ga_{0.75}Al_{0.25}As$ DHS ($\epsilon_{s1} = 12.87$ and $\epsilon_{s2} = 12.21$: $\epsilon_{s1}/\epsilon_{s2} = 1.05$) with a well width of 20 nm (a) and of 5 nm (b). It is to be seen that both image contributions, the mutual and the self-image part, have opposite sign. For small distances the magnitude of the mutual image part is nearly the same as that of the self-image part. But for larger distances the mutual image part goes to zero and hence, the self-image part dominates the whole image potential of the electron–hole interaction.

In figure 2 the interaction potential $V^{\mathrm{C}}{}_{00}(r)$ is plotted for a layered structure with $\epsilon_{s1}/\epsilon_{s2} = 1.81$ (for instance Si–CaF_2: $\epsilon_{s1} = 12.0$ and $\epsilon_{s2} = 6.63$). It is to be seen, that now the image contributions become more important as in the case $\epsilon_{s1}/\epsilon_{s2} = 1.05$. Because both image contributions have opposite sign and they are in a wide range of the same order it is necessary to include both contributions in the calculation. Hence, the neglection of the self-image contribution as done

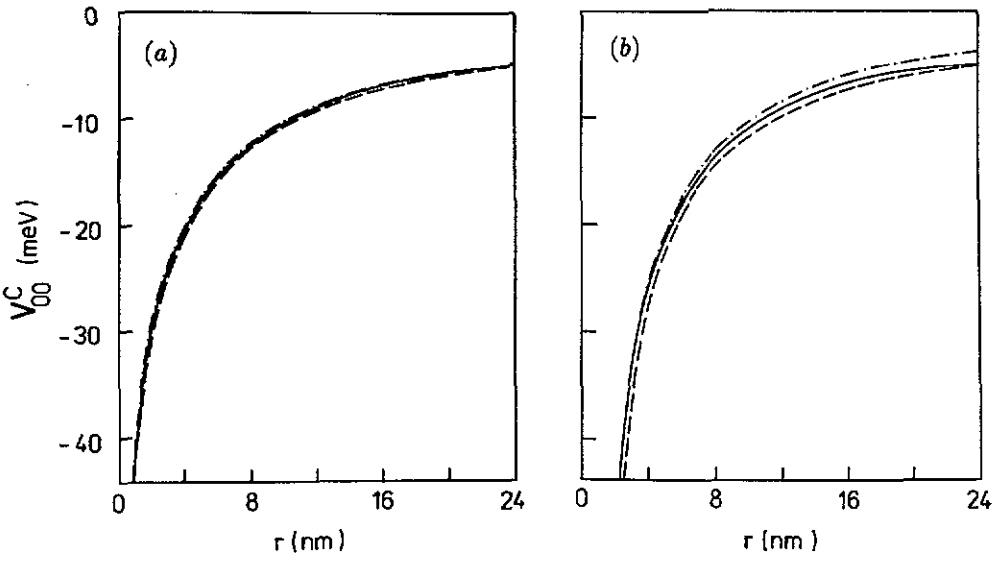

Figure 1. Electron–hole interaction potential for a GaAs–$Ga_{1-x}Al_xAs$ DHS with $\epsilon_{s1}/\epsilon_{s2} = 1.05$ without any image contribution (solid curve), without the self-image contribution (dashed curve) and with all image contributions (dashed-dotted curve) for (*a*) $a = 20$ nm and (*b*) $a = 5$ nm.

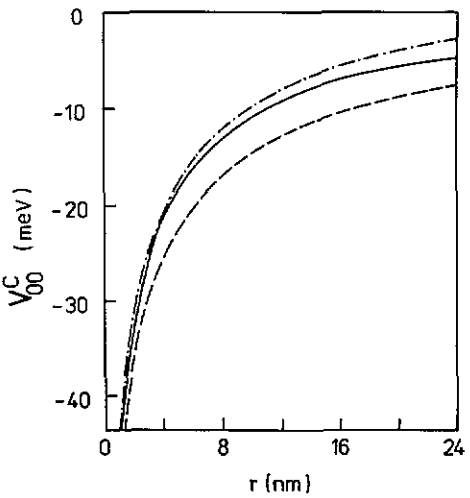

Figure 2. Electron–hole interaction potential for a DHS with $\epsilon_{s1}/\epsilon_{s2} = 1.81$ and $a = 20$ nm without any image contribution (solid curve), without the self-image contribution (dashed curve) and with all image contributions (dashed-dotted curve).

by Keldysh (1979) can give wrong results especially for layered systems with larger differencies in the background dielectric constants. We note that is possible to include the contributions of the self-image parts also as a electrostatic correction to the subband energies of electrons and holes. This is possible because the self-image terms are functions only of the dielectric constants and the thickness of the quantum well and not of the distance r between electron and hole. Following the interaction potential contains only V^{DIR} and V^{MIM} and the corresponding V^{SIM} should appear

in the single-particle equation for the electron and hole, respectively. But in this paper we are mainly interested in the action of all image forces on the electron–hole pair and hence, we include all terms. At the end of the calculation the self-image contribution may be considered as a correction to the subband energy.

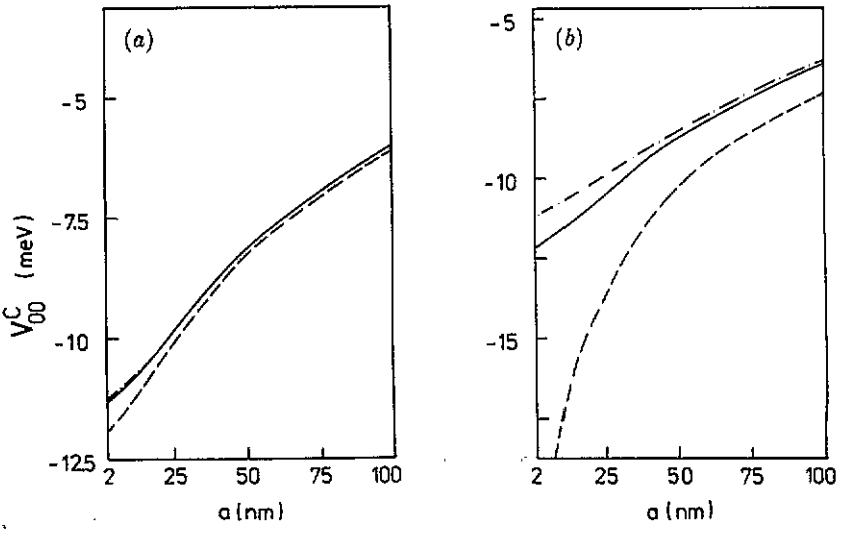

Figure 3. Electron–hole interaction potential for a DHS with (*a*) $\epsilon_{s1}/\epsilon_{s2} = 1.05$ and (*b*) $\epsilon_{s1}/\epsilon_{s2} = 1.81$ with $r = 10$ nm without any image contribution (solid curve), without the self-image contribution (dashed curve) and with all image contributions (dashed-dotted curve).

In figure 3 we have plotted $V^C{}_{00}$ versus a for a system with $\epsilon_{s1}/\epsilon_{s2} = 1.05$ (*a*) and for a system with $\epsilon_{s1}/\epsilon_{s2} = 1.81$ (*b*). It is to be seen that the dependence of $V^C{}_{00}$ on the well width is stronger for quantum wells with larger differencies of the dielectric constants. In figure 3(*b*) one can see the resulting mistake if one only includes the direct and the mutual image contribution to the interaction potential (difference between the dashed and the dashed-dotted line). Following, the result is more exact if one neglects the image parts entirely as in the case if one includes only parts of these.

In figure 4 we have plotted $V^C{}_{00}$ versus $\epsilon_{s1}/\epsilon_{s2}$ for two different distances r between electron and hole. This figure demonstrates very clearly the importance of the image effects for the electron–hole interaction potential in layered systems. It is to be seen that the magnitude of the mutual image and that of the self-image potential increase nearly equal with increasing $\epsilon_{s1}/\epsilon_{s2}$.

In figure 5 we present results for the heavy-hole exciton binding energy versus $\epsilon_{s1}/\epsilon_{s2}$. For simplicity we use $m_e, m_{h\pm}$ and $\mu_\pm$ from GaAs ($\gamma_1 = 7.36, \gamma_2 = 2.57$) to illustrate the image effects only. For GaAs the exciton Bohr radius is for the heavy-hole exciton $a_{ex+} = 17.06$ nm and for the light-hole exciton $a_{ex-} = 13.55$ nm. The corresponding effective Rydberg constant $Ry_\pm = \hbar^2/(2a_{ex\pm}{}^2\mu_\pm)$ is $Ry_+ = 3.28$ meV and $Ry_- = 4.12$ meV, respectively. It is to be seen that analogeous as for the interaction potential, the image effects to the electron–hole interaction become important for binding energy. Including all image contributions the exciton binding energy is lower than in the case without image forces. But the mutual image

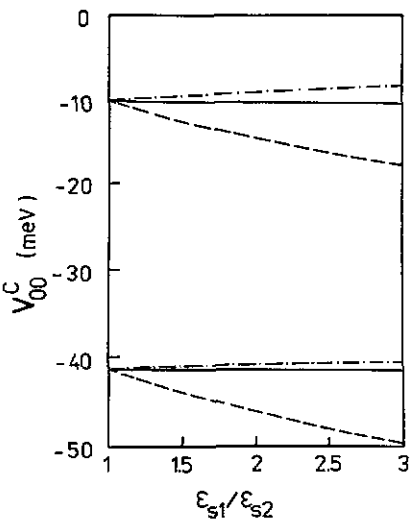

Figure 4. Electron–hole interaction potential for a DHS with a thickness of 20 nm and $r = 10$ nm (the three upper curves) and $r = 1$ nm (the three lower curves) without any image contribution (solid curve), without the self-image contribution (dashed curve) and with all image contributions (dashed-dotted curve).

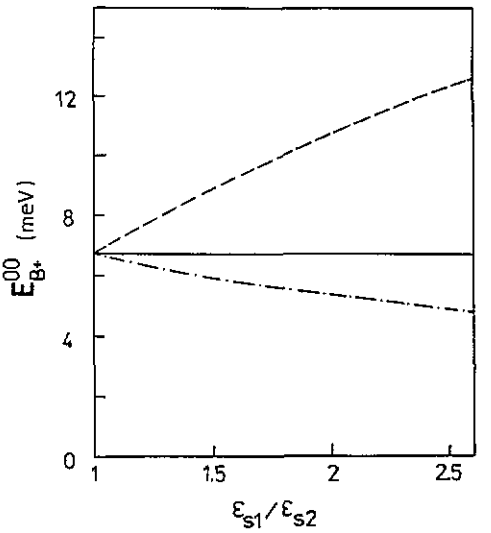

Figure 5. Exciton binding energy for a DHS without any image contribution (solid curve), without the self-image contribution (dashed curve) and with all image contributions (dashed-dotted curve) for $a = 20$ nm.

part gives rise to larger values of the binding energy. Following, if one includes the self-image parts as a correction to the subband energy and the mutual image part as a correction to the binding energy, the binding energy is increased by the image charges. This agrees well with the recent results of Andreani, Pasquarello (1990) and Tran Thoai *et al* (1990).

In conclusion we note, that the image potential effects on the excitonic properties are weak for systems with small differencies of the background dielectric constant, especially for the system GaAs–$Ga_{1-x}Al_xAs$. This is in agreement with recent calculations of the hydrogenic donor binding energy (Wendler and Hartwig 1990). But our calculations show, that it is necessary to include both image parts, the mutual and the self-image parts. The inclusion of the mutual image potential only can give wrong results, especially for systems with larger differencies in the background dielectric constants.

References

Andreani L C and Pasquarello A 1990 *Phys. Rev.* B **42** 8928
Bastard G, Mendez E E, Chang L L and Esaki L 1982 *Phys. Rev.* B **26** 1974
Brum J A and Bastard G 1985 *Phys. Rev.* B **31** 3893
Dingle R, Gossard A C and Wiegmann W 1975 *Phys. Rev. Lett.* **34** 1327
Dingle R, Wiegmann W and Henry C H 1974 *Phys. Rev. Lett.* **33** 827
Greene R L and Bajaj K K 1983 *Solid State Commun.* **45** 831
Greene R L, Bajaj K K and Phelps D E 1984 *Phys. Rev.* B **29** 1807
Keldysh L V 1979 *Pis'ma Zh. Eksp. Teor. Fiz.* **29** 716 (1979 Engl. Transl. *JETP Lett.* **29** 658)

Koteles E S and Chi J Y 1988 *Phys. Rev.* B **37** 6332
Lee Y C and Lin D L 1979 *Phys. Rev.* B **19** 1982
Meynadier M H, Delalande C, Bastard G, Voos M, Alexandre F and Lievin J L 1985 *Phys. Rev.* B **31** 5539
Miller R C, Kleinman D A and Gossard A C 1984 *Phys. Rev.* B **29** 7085
Miller R C, Kleinman D A, Tsang W T and Gossard A C 1981 *Phys. Rev.* B **24** 1134
Tran Thoai D B, Zimmermann R, Grundmann M and Bimberg D 1990 *Phys. Rev.* B **42** 5906
Wendler L, Bechstedt F and Fiedler M 1990 *Phys. Status Solidi b* **159** 143
Wendler L and Hartwig B 1990 *J. Phys.: Condens. Matter* **2** 8847
Whittaker D M and Elliot R J 1988 *Solid State Commun.* **68** 1
Wu Ji-Wei 1989 *Phys. Rev.* B **39** 12944